Wind and Structures, *Vol. 26, No. 1 (2018) 25-34*
DOI: https://doi.org/10.12989/was.2018.26.1.025

Beam finite element model of a vibrate wind blade in large elastic deformation

Hedi Hamdi*[1] and Khaled Farah[2a]

[1]Applied Mechanics and Engineering Laboratory, National Engineering School of Tunis, University of Tunis El Manar, 2092 Manar II, Tunis, Tunisia
[2]Civil Engineering Laboratory, National Engineering School of Tunis, University of Tunis El Manar, 2092 Manar II, Tunis, Tunisia

(Received May 12, 2017, Revised December 25, 2017, Accepted December 28, 2017)

Abstract. This paper presents a beam finite element model of a vibrate wind blade in large elastic deformation subjected to the aerodynamic, centrifugal, gyroscopic and gravity loads. The gyroscopic loads applied to the blade are induced by her simultaneous vibration and rotation. The proposed beam finite element model is based on a simplex interpolation method and it is mainly intended to the numerical analysis of wind blades vibration in large elastic deformation. For this purpose, the theory of the sheared beams and the finite element method are combined to develop the algebraic equations system governing the three-dimensional motion of blade vibration. The applicability of the theoretical approach is elucidated through an original case study. Also, the static deformation of the used wind blade is assessed by appropriate software using a solid finite element model in order to show the effectiveness of the obtained results. To simulate the nonlinear dynamic response of wind blade, the predictor-corrector Newmark scheme is applied and the stability of numerical process is approved during a large time of blade functioning. Finally, the influence of the modified geometrical stiffness on the amplitudes and frequencies of the wind blade vibration induced by the sinusoidal excitation of gravity is analyzed.

Keywords: vibrate wind blade; large elastic deformation; finite element method

1. Introduction

The persistent vibration of the wind blades is one of the causes of the material damage and the reducing of the wind turbine efficiency. Thereby, the realistic mechanical behavior of the wind blades subjected to the non-stationary loads should be predicted. In the last decade, a numerous theoretical models dealing with the wind blades vibration are proposed. These models are formulated using various methods like the beam finite element method by assimilating the blade to a cantilever beam. The theoretical concepts of the beam finite element method are based on the beams theory and the finite element method in order to reduce the order of the computing model. The numerical analysis of the nonlinear systems is more stable and reliable when the finite element model of structure is reduced. Indeed, the beam finite element model is commonly used in the nonlinear dynamic analysis of wind blades.

The Timoshenko beams theory taking into account the transverse shear has applied by Stoykov and Ribeiro (2013) to analyze the nonlinear vibration of rotating beams in linear elastic material. The geometric nonlinearity is due to the large elastic deformation of the beams. Generally, this theory is applied to the thick beams such as the wind blades. Using the same theory Rao and Gupta (2001) have studied the vibration modes of the tapered and twisted beams. The effects of twist angle and the rotation speed on the vibration modes of a rotating cantilever beam are revealed. However the gyroscopic effect due to the simultaneous beam rotation and vibration is not considered. Rezaei *et al*. (2015) have developed a reduced order model to predict the dynamic response of wind blades in large elastic deformation under the aerodynamic and gravitational loads. Their modeling is based on the Euler-Bernoulli beams theory neglecting the transverse shear. They have approved that the torsional beating of wind blade is strongly influenced by the geometric stiffness of the large elastic deformation of blade.

The theoretical models are established to analyze and solve the technological problems. In this context; Ponta *et al*. (2016) showed the negative effect of the blade cyclic deformation on the wind turbine efficiency. Ghasemi *et al.* (2014) have studied the aeroelastic stability of an original wind blade. They have approved that the coupling of bending and torsional vibration of wind blades is a major cause of their instability and damaging. Ashrafi *et al.* (2015) have studied the pitch control system integrated in the modern wind rotors to optimize her power output. To evaluate the wind loads, the blade element momentum theory is used. In other side, Wang *et al*. (2014) implement a detection process of the structural damages of wind blades based on the dynamics analysis using the finite element method. Dotti *et al*. (2016) have simulated the dynamic response of a thin-walled beam with a breathing crack and subjected to a sinusoidal excitation. The topological changes of the dynamic response allow identifying the breathing crack location. To reduce the fatigue of wind blades, Lee *et al.* (2013) have studied the implement of the active aerodynamic load control devices based on a proportional derivative controller. Also, Staino and Basu

*Corresponding author, Associate Professor
E-mail: hedi.hamdi@isetr.rnu.tn
[a] Associate Professor
khaled.farah@isetgf.rnu.tn

Copyright © 2018 Techno-Press, Ltd.
http://www.techno-press.com/journals/was&subpage=7 ISSN: 1226-6116 (Print), 1598-6225 (Online)

(2013) proposed an analytical modeling and control of wind blade vibration due to change in the rotational speed.

In this paper, a beam finite element model is formulated considering the large elastic deformation of the sheared beams. Then, the proposed model is applied to simulate the dynamic response of a rotating wind blade at a constant angular speed and subjected to the sinusoidal excitation of gravity. The gyroscopic loads due to the simultaneous blade rotation and vibration are taken into account. The aerodynamic and centrifugal loads are considered and supposed stationary at the time of simulation. Finally, the influence of the large elastic deformation stiffness on the amplitudes and frequencies of the blade vibration are analyzed.

2. The proposed model

The wind blade is assimilated to a cantilever beam with a variable cross-section. The blade material is assumed homogeneous and isotropic. Also, a linear elastic behavior of the blade material is considered. The three-dimensional vibration motion of an infinitesimal blade element (see Fig. 1) is described by their all degrees of freedom: u, v, w, α, β and γ. Then, we applied the beam finite element method to develop the algebraic equations system governing the vibration blade motion in large elastic deformation as follows

$$\boldsymbol{M_e}\,\ddot{\boldsymbol{q}}_{\boldsymbol{e}} + \boldsymbol{C_e}\,\dot{\boldsymbol{q}}_{\boldsymbol{e}} + \boldsymbol{K_e q_e} + \boldsymbol{K_{ge} q_e} = \boldsymbol{F_e(t)} \tag{1}$$

The elementary stiffness K_e, mass M_e, gyroscopic C_e matrices and the applied loads vector F_e are given by Hamdi *et al*. (2014).

This study aims to formulate the geometrical stiffness matrix K_{ge} due to the large elastic deformation of the rectilinear beams. In the following, the matrices and vectors are expressed in the (x,y,z) referential related to the blade.

2.1 Geometric stiffness

The beams geometrical stiffness in the large elastic deformation is formulated using the strain energy method. By considering x-axis long beam, the components: σ_{yy}, σ_{yz} and σ_{zz} of the stress tensor are negligible in comparison with the other components: σ_{xx}, σ_{xy} and σ_{xz}. Consequently, the function of the strain energy due to the nonlinear part of the total elastic deformation of a beam finite element is expressed as follows

$$U_e = \tfrac{1}{2}\int_{V_e}\left(\sigma_{xx}\varepsilon_{xx}(\mathrm{nl}) + 2\sigma_{xy}\varepsilon_{xy}(\mathrm{nl}) + 2\sigma_{xz}\varepsilon_{xz}(\mathrm{nl})\right)dV \tag{2}$$

The strain tensor components of the deformable solids in large elastic deformation are expressed by

$$\varepsilon_{ab} = \tfrac{1}{2}\left(u_{a,b} + u_{b,a}\right) + \tfrac{1}{2}\left(u_{c,a}u_{c,b}\right) \tag{3}$$

The indices a, b and c take the letters x, y or z.

The displacement vector u of an arbitrary point $P(x,y,z)$ located on the beam cross-section is obtained as follows

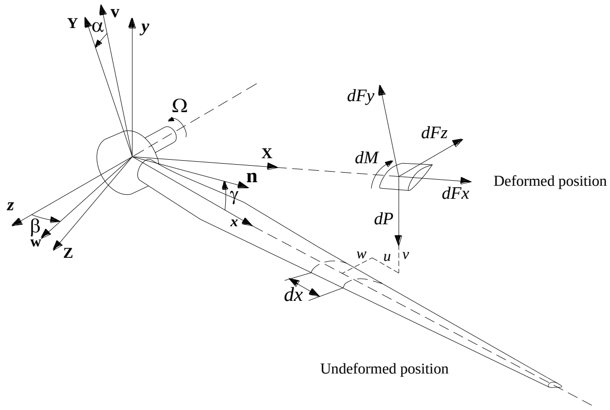

Fig. 1 Vibration motion parameters of an infinitesimal blade element and the applied loads

$$\boldsymbol{u} = \left((u + z\beta - y\gamma),\ (v - z\alpha),\ (w + y\alpha)\right)^{\mathrm{T}} \tag{4}$$

From the Eqs. (3) and (4), we obtain the linear and nonlinear parts of the strain tensor components at the point P

$$\varepsilon_{xx}(\mathrm{l}) = u_{,x} - y\gamma_{,x} + z\beta_{,x} \tag{5}$$

$$2\varepsilon_{xy}(\mathrm{l}) = v_{,x} - z\alpha_{,x} - \gamma \tag{6}$$

$$2\varepsilon_{xz}(\mathrm{l}) = w_{,x} + y\alpha_{,x} + \beta \tag{7}$$

$$\varepsilon_{xx}(\mathrm{nl}) = \tfrac{1}{2}\left((u_{,x} - y\gamma_{,x} + z\beta_{,x})^2 + (v_{,x} + z\alpha_{,x})^2 + (w_{,x} + y\alpha_{,x})^2\right) \tag{8}$$

$$2\varepsilon_{xy}(\mathrm{nl}) = \alpha(w_{,x} + y\alpha_{,x}) - \gamma(u_{,x} - y\gamma_{,x} + z\beta_{,x}) \tag{9}$$

$$2\varepsilon_{xz}(\mathrm{nl}) = \beta(u_{,x} - y\gamma_{,x} + z\beta_{,x}) - \alpha(v_{,x} + z\alpha_{,x}) \tag{10}$$

To apply the finite element method, the blade is discretized in several beam finite elements (see Fig. 2) connected by consecutive nodes. Then, we can evaluate any function φ in terms of these nodal values (φ_i and $\varphi_{j=i+1}$) by simplex isoparametric interpolation as follows

$$\varphi(\xi) = N_1(\xi)\varphi_i + N_2(\xi)\varphi_j \tag{11}$$

The function φ is: u, v, w, α, β, γ or x.

The used interpolation functions are linear

$$N_1(\xi) = (1-\xi)/2 \quad \text{and} \quad N_2(\xi) = (1+\xi)/2 \tag{12}$$

Where, ξ is the interpolation parameter variable between -1 and 1.

The gradient of the function φ with respect x is written

$$\varphi_{,x} = (\varphi_j - \varphi_i)/2 \tag{13}$$

By interpolation, the nonlinear strain tensor components can be expressed again from the Eqs. (8)-(10) by the following relations

$$\varepsilon_{xx}(\mathrm{nl}) = \boldsymbol{q}_e^{\mathrm{T}} \boldsymbol{X} \boldsymbol{q}_e;\quad 2\varepsilon_{xy}(\mathrm{nl}) = \boldsymbol{q}_e^{\mathrm{T}} \boldsymbol{Y} \boldsymbol{q}_e;\quad 2\varepsilon_{xz}(\mathrm{nl}) = \boldsymbol{q}_e^{\mathrm{T}} \boldsymbol{Z} \boldsymbol{q}_e \tag{14}$$

The X, Y and Z matrices are given by Hamdi *et al*. (2012).

The nodal displacement vector q_e of any beam finite element is

$$\boldsymbol{q_e} = (u_i,\ v_i,\ w_i,\ \alpha_i,\ \beta_i,\ \gamma_i,\ u_j,\ v_j,\ w_j,\ \alpha_j,\ \beta_j,\ \gamma_j)^{\mathbf{T}} \tag{15}$$

The function of strain energy Eq. (2) due to the nonlinear part of the total elastic deformation is expressed again using the Hooke low as follows

$$U_e = \tfrac{1}{2} \boldsymbol{q_e}^{\mathrm{T}} \underbrace{\left[\int_{V_e} \left(E\boldsymbol{X}\varepsilon_{xx} + 2G\boldsymbol{Y}\varepsilon_{xy} + 2G\boldsymbol{Z}\varepsilon_{xz} \right) dS dx \right]}_{\boldsymbol{K}_{ge}} \boldsymbol{q_e} \tag{16}$$

From the Eq. (16) we identify the geometrical stiffness matrix K_{ge} of the beam. After interpolation and negligence of the product terms of nodal displacements components, the geometrical stiffness matrix can be simplified as

$$\begin{aligned} \boldsymbol{K_{ge}} = \int_S \ & [E[(u_j - u_i) + z(\beta_j - \beta_i) - y(\gamma_j - \gamma_i)]\boldsymbol{X} + \\ & G[(v_j - v_i) - z(\alpha_j - \alpha_i)]\boldsymbol{A}_1 - G(\gamma_i \boldsymbol{A}_2 + \gamma_j \boldsymbol{A}_3) + \\ & G[(w_j - w_i) + y(\alpha_j - \alpha_i)]\boldsymbol{B}_1 - G(\beta_i \boldsymbol{B}_2 + \beta_j \boldsymbol{B}_3)]dS \end{aligned} \tag{17}$$

The constant matrices A and B depend only on the y, z and the length l of beam finite element

$$\begin{aligned} \boldsymbol{A}_1 &= \int_{-1}^{1} \boldsymbol{Y} d\xi;\quad \boldsymbol{A}_2 = \frac{l}{2}\int_{-1}^{1} N_1 \boldsymbol{Y} d\xi;\quad \boldsymbol{A}_3 = \frac{l}{2}\int_{-1}^{1} N_2 \boldsymbol{Y} d\xi; \\ \boldsymbol{B}_1 &= \int_{-1}^{1} \boldsymbol{Z} d\xi;\quad \boldsymbol{B}_2 = \frac{l}{2}\int_{-1}^{1} N_1 \boldsymbol{Z} d\xi;\quad \boldsymbol{B}_3 = \frac{l}{2}\int_{-1}^{1} N_2 \boldsymbol{Z} d\xi \end{aligned} \tag{18}$$

The geometrical stiffness matrix is function of the nodal displacements components. Consequently the governing equations system Eq. (1) is geometrically nonlinear.

2.2 Applied loads

During its operation, the wind blade is subjected to the aerodynamic, centrifugal, gyroscopic and gravity loads. The aerodynamic and the centrifugal loads are supposed stationary at the time of simulation. To calculate the aerodynamic loads in each node of blade, we use an iterative calculation algorithm developed by Dai *et al*. (2011) based on the blade element momentum theory. The gravity excitation of the rotating blade is sinusoidal and causes a harmonic vibration of blade. Indeed the simultaneous vibration and rotation of the blade generate gyroscopic torsion and bending moments. The elementary applied loads (see Fig. 1) are expressed as follows

– Aerodynamic loads of wind:

$$\begin{aligned} dFy &= \tfrac{1}{2}\rho_a C_y c V_{\mathrm{r}}^2 dx; \\ dFz &= \tfrac{1}{2}\rho_a C_z c V_{\mathrm{r}}^2 dx; \\ dM &= \tfrac{1}{2}\rho_a C_m c^2 V_{\mathrm{r}}^2 dx \end{aligned} \tag{19}$$

– Excitation force of gravity

$$d\boldsymbol{P} = -\rho g S \left(\cos\delta \sin(\Omega t),\ \cos\delta \cos(\Omega t),\ \sin\delta \right)^{\mathrm{T}} dx \tag{20}$$

– Centrifugal force of rotation

$$dFx = \rho x \Omega^2 S dx \tag{21}$$

– Gyroscopic torsion moment

$$dC_t = \rho I_{yz} \Omega^2 dx \tag{22}$$

3. Results and discussion

3.1 Study case

The proposed modeling is applied to study the static and dynamic response of a small scale wind blade (see Fig. 2) in large elastic deformation. This wind blade is designed and manufactured by Habali and Saleh (2000a, b) for a 15 kW wind turbine. Due to its aerodynamic performance, the NACA-63-621 airfoil type of the blade working region is chosen by the designers. The practice test have approved that her optimal operation is reached when the wind speed is 10 m/s and the rotation speed is 9.17 rad/s. The model inputs are summarized in the Tables 1-3.

3.2 Static response

The iterative Newton method is used to evaluate the static displacements components of the blade axis (see Figs. 3(a)-3(d)) under the stationary loads. We note the static displacement components of the blade are weak reduced by the geometric stiffness of the large elastic deformation. Particularly, the angular of the blade torsion is more influenced by this stiffness. During rotation, the blade starts to vibrate around this static position under the gravity excitation.

In order to validate the proposed beam finite element model, we simulate the static deformation of the studied blade using the SolidWorks software with the large deformation option. The stationary loads are distrubed along the blade axis (see Fig. 4(b)) in accordance with Table 3. In the same way, Domnica *et al*. (2016) have applied the wind loads to study a wind blade. Subsequently a volumetric meshing of the blade (see Fig. 4(a)) is automatically created when the static study is carried out.

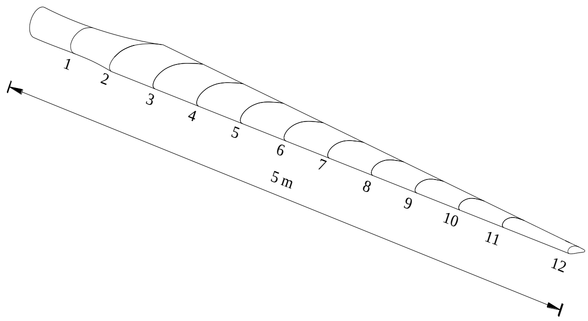

Fig. 2 Small scale wind blade discretized in twelve beam finite elements

Table 1 Mechanical properties of the used wind blade

Parameters	Descriptions	Values
ρ	Mass density of the blade	1400 kg/m3
E	Elasticity modulus of material	6000 MPa
G	Shear modulus of material	2542 MPa
R	Rotor radius	5.45 m
δ	Rotor tilt angle	12 deg
g	Gravity modulus	9.81 N/Kg
ρ_a	Density of air	1.25 kg/m3
V	Wind speed	10 m/s
Ω	Rotor angular speed	9.17 rad/s

Table 2 Geometrical properties of the beam finite elements

Element	l(mm)	c(mm)	S(mm^2)	I_{xx}(cm^4)	I_{yy}(cm^4)	I_{zz}(cm^4)	I_{yz}(cm^4)
1	400	210	8193	7510	4153	3357	-363
2	400	504	8552	22630	18070	4566	-5240
3	400	600	11368	32920	27960	4965	-8450
4	400	562	10514	26520	22820	3698	-6797
5	400	524	9741	21190	17990	3204	-5626
6	400	486	8897	16610	13940	2678	-4565
7	400	448	8137	12750	10600	2146	-3607
8	400	410	7293	9576	7845	1731	-2807
9	400	371	6510	6944	5578	1365	-2124
10	400	333	5713	4845	3798	1047	-1555
11	400	295	4968	3250	2465	786	-1096
12	600	257	3885	1872	1344	528	-673

The solid finite elements of the software model are tetrahedron type of four nodes with three degrees of freedom per node. In contrast, our finite element model uses beam elements of two nodes with six degrees of freedom per node decreasing the total number of the structure freedom degrees compared to the software modeling.

The simulation results are the displacement and the deformation fields (see Figs. 5(a) and 5(b)) of the blade structure. The maximum value of the resultant displacement obtained by the SolidWorks software is 25 mm; on the other hand the value evaluated by the proposed model is about 21 mm for the wind speed 10 m/s. A similarly static study of the adopted wind blade was carried out by Habali and Saleh (2000a) using solid finite element model. According to their results, the maximum displacement of the blade is in order 100 mm for the extreme wind speed 42 m/s. Assuming that the static deformation variation of blade is quasi-linearly as wind speed increases, it should be noted that the obtained numerical values are valid.

Table 3 Stationary loads values at each node of the blade

Node	*x*(m)	*Fx*(N)	*Fy*(N)	*Fz*(N)	*Pz*(N)	*M*(Nm)	C_t(Nm)
1	0.85	376.9	13.36	-11.18	-10.58	-3.26	-2.5
2	1.25	644.7	19.84	-11.08	-12.41	-4.54	-3.2
3	1.65	873.4	27.54	-10.93	-12.86	-3.87	-3.6
4	2.05	1015.3	35.97	-10.48	-12.04	-3.19	-2.9
5	2.45	1120.3	44.66	-9.72	-11.11	-2.87	-2.4
6	2.85	1195.5	53.10	-8.66	-10.19	-2.65	-1.9
7	3.25	1240.8	60.66	-7.35	-9.27	-2.43	-1.5
8	3.65	1254.8	67.19	-5.91	-8.35	-1.71	-1.2
9	4.05	1239.6	72.14	-4.37	-7.43	-1.56	-0.9
10	4.45	1198.6	75.22	-2.83	-6.54	-1.33	-0.6
11	4.85	1183.9	77.51	-1.23	-6.99	-1.05	-0.5
12	5.45	821.5	38.75	-0.61	-3.95	-1.02	-0.2

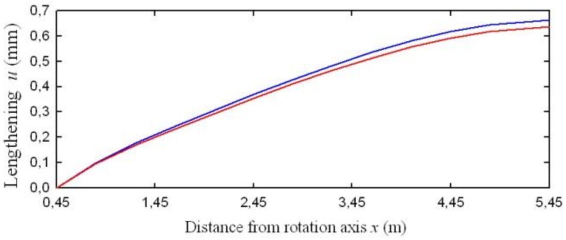

(a) Lengthening of the blade

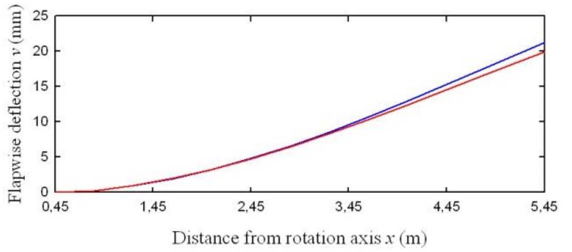

(b) Flapwise deflection of the blade

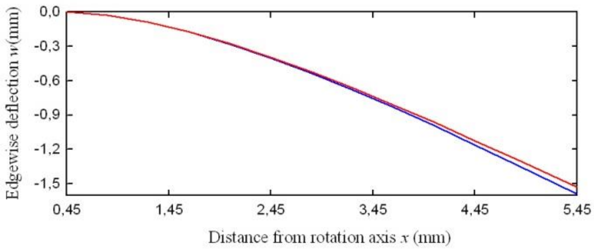

(c) Edgewise deflection of the blade

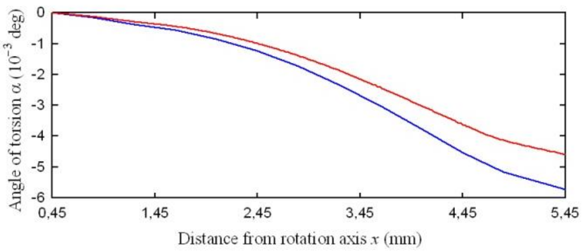

(d) Blade angle torsion

Fig. 3 Static displacement components of the blade axis in cases: small elastic deformation (curves in blue) and large elastic deformation (curves in red)

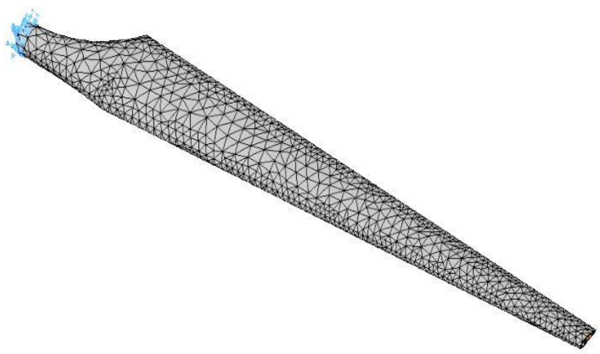

(a) Volumetric meshing of the blade

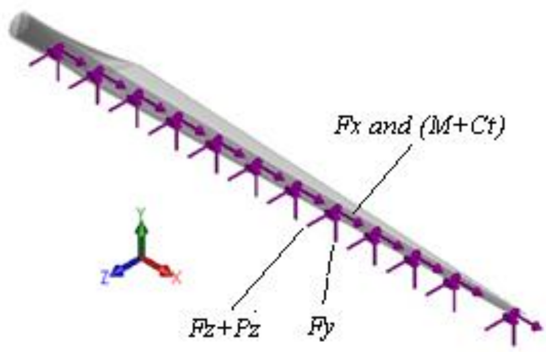

(b) Distribution of the applied loads on the blade

Fig. 4 Volumetric meshing of the used blade and loads distribution

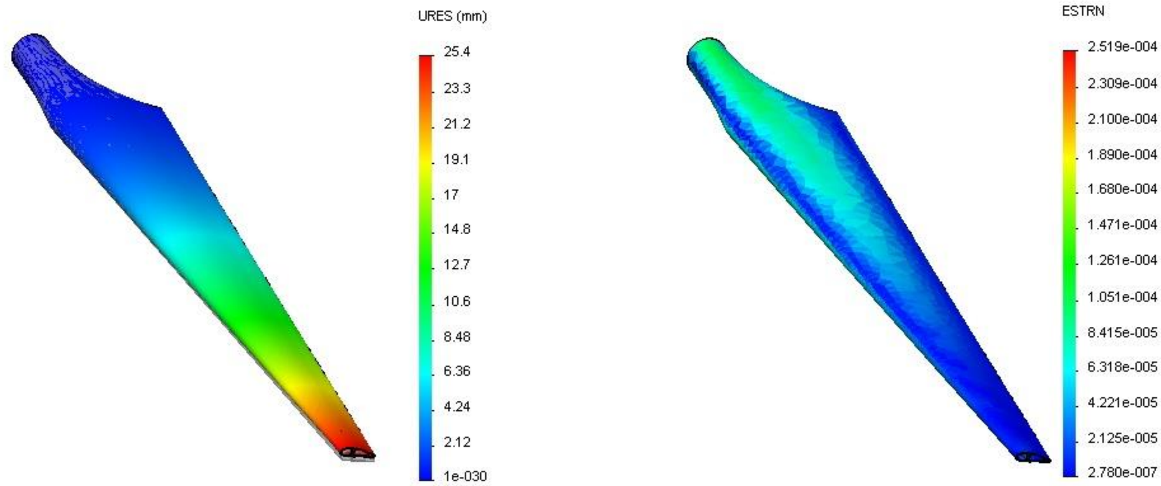

(a) Displacement field (b) Deformation field

Fig. 5 Simulation results of the blade structure by SolidWorks software

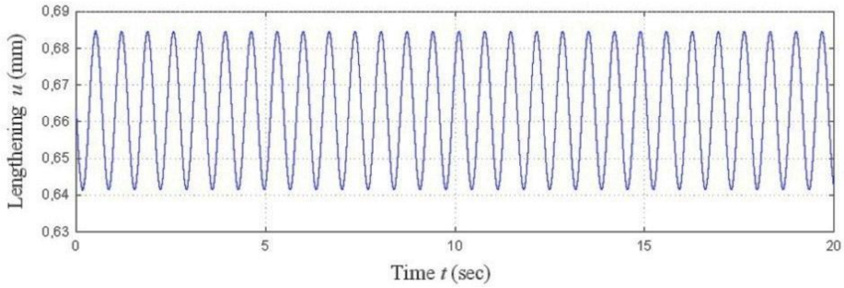

Fig. 6 Lengthening of the blade

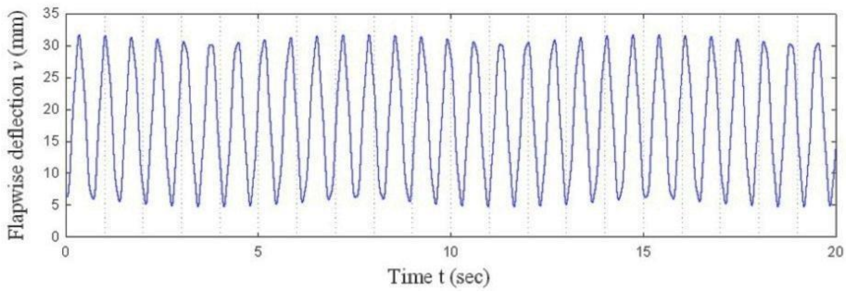

Fig. 7 Flapwise deflection of the blade in small elastic deformation case

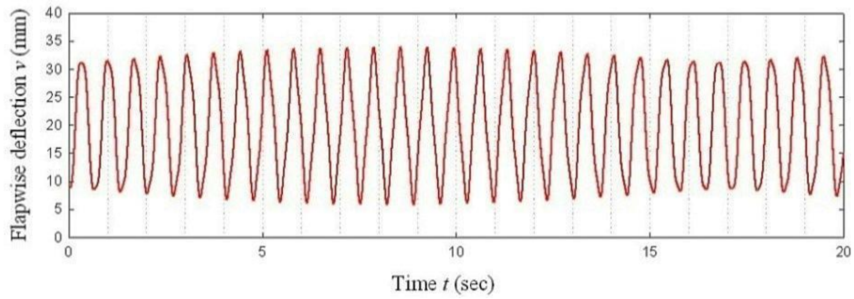

Fig. 8 Flapwise deflection of wind blade in large elastic deformation case

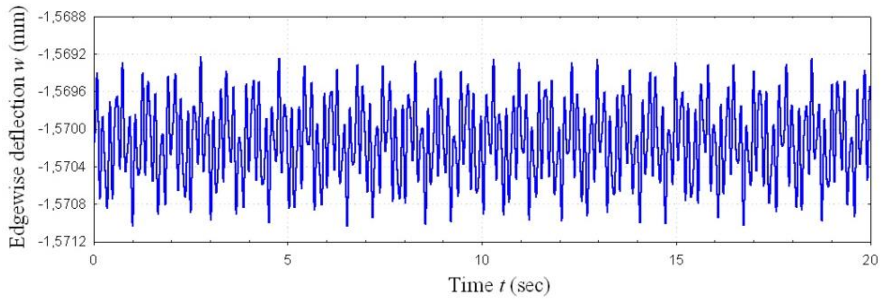

Fig. 9 Edgewise deflection of wind blade in small elastic deformation case

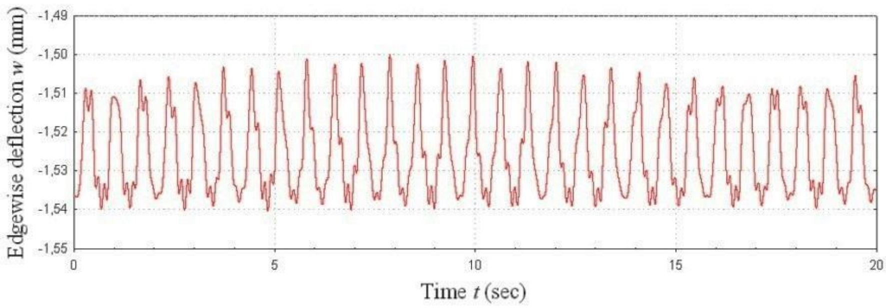

Fig. 10 Edgewise deflection of wind blade in large elastic deformation

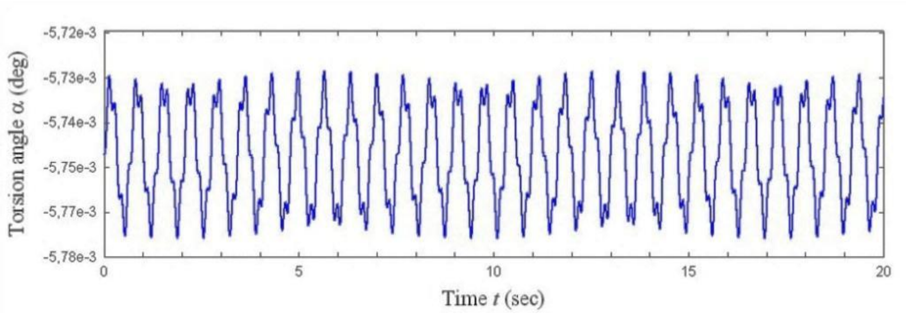

Fig. 11 Torsion angle of the wind blade in small elastic deformation

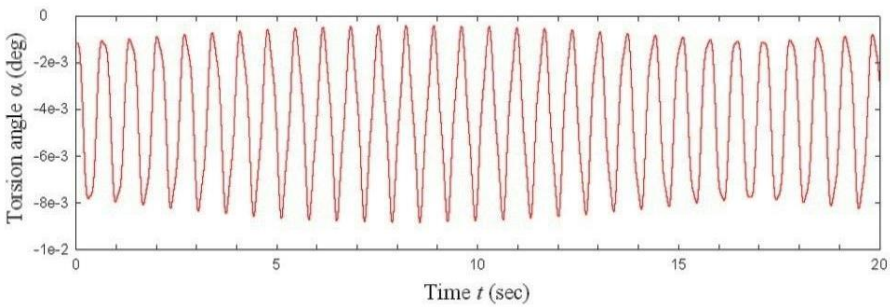

Fig. 12 Torsion angle of the wind blade in large elastic deformation

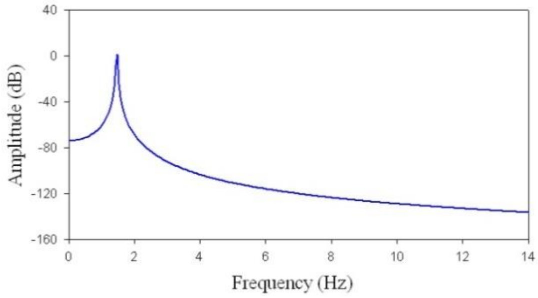

(a) FFT of $u(t)$

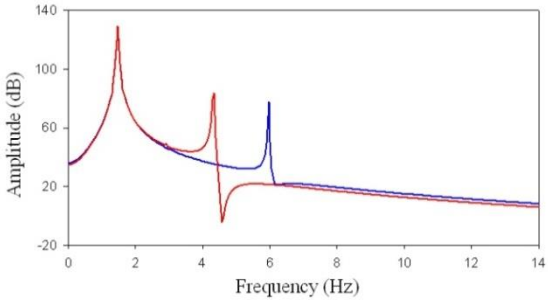

(b) FFT of $v(t)$

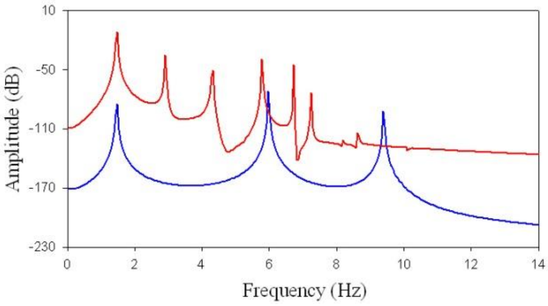

(c) FFT of w(t)

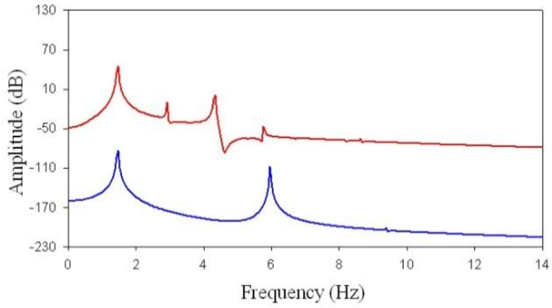

(d) FFT of α(t)

Fig. 13 FFT of the dynamic response components in cases: small elastic deformation (curves in blue) and large elastic deformation (curves in red)

3.3 Dynamic response

To simulate the nonlinear dynamic response of the wind blade under the excitation of gravity, a MATLAB code using predictor-corrector Newmark scheme is established. In the nonlinear dynamic case (large elastic deformation), the stability of the simulation process with a constant time step (10^{-5} s) is approved during a large time (20 s) of blade functioning. The dynamic response components at the end node of the blade are showed in Figs. 6-12. We note the amplitude of flapwise vibration is higher than the edgewise vibration component. Indeed, the flapwise component of wind blade vibration may be causes the damage of the structure. Moreover the flapwise component is not heavily influenced by the geometrical stiffness of large deformation like the other components of blade vibration. The torsion vibration component (see Figs. 11 and 12) is due to the simultaneous blade rotation and vibration. The torsional vibration amplitude is clearly amplified by the geometric stiffness of the large elastic deformation. However the lengthening of the blade is not influenced by this stiffness.

The frequency spectrums shown in Fig. 13 are obtained by the Fast Fourier Transform (FFT) of the blade dynamic response components. The first frequency of the blade vibration corresponds to the rotor rotation speed because the structural damping is neglected in the modeling. It is clear that the amplitudes of the blade vibration components are increased and her first frequencies are reduced by the geometrical stiffness of large elastic deformation.

4. Conclusions

In this study a beam finite element model is developed based on a simplex interpolation method. Then, it is applied to analyze the nonlinear dynamic response of wind blade in large elastic deformation. The proposed approach allows assessing the lengthening, deflection and torsion of the blade structure. The aerodynamic and centrifugal loadings are applied to the blade. Also, the gyroscopic loads induced by the simultaneous blade rotation and vibration are considered. In the first part, the simulation of the static deformation of a small scale wind blade under the stationary loads was carried out by standard software using solid finite element model in order to check the obtained results. In the second part, the dynamic response components of the wind blade subjected to the excitation of gravity is simulated and the stability of the numerical process is approved during a large time of blade functioning.

Based on the obtained results, we conclude that the value of the static deformation of the wind blade is weakly reduced by the geometric stiffness of large elastic deformation, but its dynamic response is clearly influenced. Furthermore, the geometric stiffness of the large elastic deformation increases the amplitude of the wind blade vibration and reduces her frequencies. Finally, the torsional vibration amplitude of the wind blade generated by the gyroscopic effect is clearly amplified by the geometric stiffness of the large elastic deformation. Therefore, the risk of damaging of the blade structure is increases.

References

Ashrafi, Z.N., Ghaderi, M. and Sedaghat, A. (2015), “Parametric study on off-design aerodynamic performance of a horizontal axis wind turbine blade and proposed pitch control”, *Energ. Convers. Manage*., **93**, 349-356.

Dai, J.C., Hu, Y.P., Liu, D.S. and Long, X. (2011), “Aerodynamic loads calculation and analysis for large scale wind turbine based on combining BEM modified theory with dynamic stall model”, *Renew. Energ.*, **36**(3), 1095-1104.

Domnica, S.M., Ioan, C. and Ionut, T. (2016), “Structural optimization of composite from wind turbine blades with horizontal axis using finite element analysis”, *Procedia Technol*., **22**, 726-733.

Dotti, F.E., Cortínez, V.H. and Reguera, F. (2016), “Non-linear dynamic response to simple harmonic excitation of a thin-walled beam with a breathing crack”, *Appl. Math. Model.*, **40**(1), 451-467.

Ghasemi, A.R., Jahanshir, A. and Tarighat, M.H. (2014), “Numerical and analytical study of aeroelastic characteristics of wind turbine composite blades”, *Wind Struct.*, **18**(2), 103-116.

Habali, S.M. and Saleh, I.A. (2000a), “Local design, testing and manufacturing of small mixed airfoil wind turbine blades of glass fiber reinforced plastics: part I: design of the blade and root”, *Energ. Convers. Manage*., **41**(3), 249-280.

Habali, S.M. and Saleh, I.A. (2000b), “Local design, testing and manufacturing of small mixed airfoil wind turbine blades of glass fiber reinforced plastics: Part II: Manufacturing of the blade and rotor”, *Energ. Convers. Manage*., **41**(3), 281-298.

Hamdi, H., Mrad, C. and Nasri, R. (2012), “Effects of gyroscopic coupling on the dynamics of a wind turbine blade with horizontal axis”, In *Condition Monitoring of Machinery in Non-Stationary Operations*, 159-174. Springer Berlin Heidelberg.

Hamdi, H., Mrad, C., Hamdi, A. and Nasri, R. (2014), “Dynamic response of a horizontal axis wind turbine blade under aerodynamic, gravity and gyroscopic effects”, *Appl. Acoust.*, **86**, 154-164.

Lee, J.W., Kim, J.K., Han, J.H. and Shin, H.K. (2013), “Active load control for wind turbine blades using trailing edge flap”, *Wind Struct*., **16**(3), 263-278.

Ponta, F.L., Otero, A.D., Lago, L.I. and Rajan, A. (2016), “Effects of rotor deformation in wind-turbine performance: The dynamic rotor deformation blade element momentum model (DRD–BEM)”, *Renew. Energ.*, **92**, 157-170.

Rao, S.S. and Gupta, R.S. (2001), “Finite element vibration analysis of rotating Timoshenko beams”, *J. Sound Vib*., **242**(1), 103-124.

Rezaei, M.M., Behzad, M., Haddadpour, H. andMoradi, H. (2015), “Development of a reduced order model for nonlinear analysis of the wind turbine blade dynamics”, *Renew. Energ.*, **76**, 264-282.

Staino, A. and Basu, B. (2013), “Dynamics and control of vibrations in wind turbines with variable rotor speed”, *Eng. Struct*., **56**, 58-67.

Stoykov, S. and Ribeiro, P. (2013), “Vibration analysis of rotating 3D beams by the p-version finite element method”, *Finite Elem. Anal. Des.*, **65**, 76-88.

Wang, Y., Liang, M. and Xiang, J. (2014). « Damage detection method for wind turbine blades based on dynamics analysis and mode shape difference curvature information”, *Mech. Syst. Signal Pr.*, **48**(1), 351-367.

CC

Nomenclature

$(..)_{,x}$	Partial derivative of the function (..) with respect x
U_e	Strain energy function of the nonlinear elastic deformation
$\boldsymbol{K}_{\mathrm{ge}}$	Geometrical stiffness matrix
$\boldsymbol{K}_{\mathrm{e}}$	Mechanical stiffness matrix
$\boldsymbol{M}_{\mathrm{e}}$	Mass matrix
$\boldsymbol{C}_{\mathrm{e}}$	Gyroscopic matrix
$\boldsymbol{F}_e$	Loads vector
$\boldsymbol{q}_{\mathrm{e}}$	Nodal displacements vector
$\boldsymbol{u}$	Displacements vector of an arbitrary point of blade
σ_{xx}	Normal stress to the cross section
σ_{xy}	Shear stress to the cross section in y direction
σ_{xz}	Shear stress to the cross section in z direction
ε_{xx}	Total longitudinal strain in x direction
ε_{xy}	Total shear strain in y direction
ε_{xz}	Total shear strain in z direction
$\varepsilon_{xx}(\mathrm{nl})$	Nonlinear part of longitudinal strain in x direction
$\varepsilon_{xy}(\mathrm{nl})$	Nonlinear part of transverse strain in y direction
$\varepsilon_{xz}(\mathrm{nl})$	Nonlinear part of transverse strain in z direction
$\varepsilon_{xx}(\mathrm{l})$	Linear part of longitudinal strain in x direction
$\varepsilon_{xy}(\mathrm{l})$	Linear part of shear strain in y direction
$\varepsilon_{xz}(\mathrm{l})$	Linear part of shear strain in z direction
$u, v, w, \alpha, \beta, \gamma$	Degrees of freedom of the blade element
$I_{xx}, I_{yy}, I_{zz}, I_{yz}$	Quadratic inertia moments of the cross section
N_1, N_2	Two interpolation functions
x, y, z	Coordinates of an arbitrary point of the blade
i, j	Indices of two consecutives nodes
ξ	Interpolation parameter
E	Elasticity modulus of material
G	Shear modulus of material
ρ	Density of material
ρ_{a}	Density of air
$\boldsymbol{\Omega}$	Angular speed of blade
V_{r}	Relative speed of wind
Fx	Centrifugal force
Fy	Aerodynamic force in y direction
Fz	Aerodynamic force in z direction
M	Aerodynamic moment of torsion
C_t	Gyroscopic moment of torsion
$\boldsymbol{P}$	Gravity force vector
C_{y}	Aerodynamic coefficient in y direction
C_{z}	Aerodynamic coefficient in z direction
C_{m}	Aerodynamic moment coefficient
g	Gravity modulus
S	Cross section area
δ	Rotor tilt angle
c	Chord of cross section
l	Beam element length
t	Time